

## Single-pole double-throw-type optomechanically induced transparency

Zhi-Xiang Su , Ai-Dong Zhu, and Lin Yu \*

*Department of Physics, College of Science, Yanbian University, Yanji, Jilin 133002, China*



(Received 29 March 2024; accepted 11 July 2024; published 1 August 2024)

We propose a scheme for achieving twofold nonreciprocal optomechanically induced transparency (OMIT) in a three-cavity optomechanical system. In this system, an optical microring resonator is evanescently coupled to two microring optomechanical resonators simultaneously, and a beam splitter is utilized to establish two distinct optical paths. By utilizing a strong control laser and a weak probe laser to drive the resonators, a twofold nonreciprocal OMIT phenomenon can be observed. Specifically, the distinct propagation direction of the control laser will result in nonreciprocal OMIT in the two different paths, respectively. In contrast to two-cavity optomechanical systems, the OMIT can be significantly enhanced through indirect coupling, resulting in an  $\sim 23.4\%$  increase at the frequency resonance. This unique structure of a three-cavity system renders it an ideal optical single-pole double-throw (SPDT) switch or an ideal optical SPDT-like isolator, which can play an pivotal role in optical communication networks and present exciting opportunities in quantum technologies.

DOI: [10.1103/PhysRevA.110.023502](https://doi.org/10.1103/PhysRevA.110.023502)

### I. INTRODUCTION

Cavity optomechanics [1], which investigates the interaction between light fields and mechanical motion, has received increasing attention for the broad applications in testing macroscopic quantum physics, high-precision measurements, and quantum information processing [1–5]. Various systems have been proposed for investigating such interactions, such as Fabry-Pérot cavities [6,7], whispering-gallery microcavities [8–10], membrane-in-the-middle systems [11–14], and superconducting circuits [15,16]. In these optomechanical systems, the radiation pressure forces induce mechanical modes, which in turn affect the optical properties, resulting in remarkable quantum effects, such as the ground-state cooling of mechanical modes [17–22], quantum entanglement [23–26], normal mode splitting [27–29], chaotic dynamics [30–32], optomechanically induced transparency (OMIT) [33], etc.

OMIT, a significant characteristic in cavity photomechanics, can be considered as an analog to the electromagnetically induced transparency (EIT) observed in atomic systems. The physical mechanism underlying this phenomenon can be described as follows: The optomechanical interaction induces control light to scatter Stokes and anti-Stokes photons. Within a resolved-sideband regime, Stokes scattering is strongly suppressed due to its high off-resonance with the optical cavity. As a result, only an anti-Stokes field accumulates within this cavity. The destructive interference between anti-Stokes photons and probe photons effectively hinders the accumulation of probe photons within the cavity. Therefore, the transmission spectrum of the probe light appears as a transparent window near the frequency resonance. The phenomenon was initially theoretically predicted by Agarwal and Huang [33], and subsequently experimentally

demonstrated by Weis *et al.* [34]. Since then, relevant scholars have embarked on extensive research into this physical property. In the process, nonreciprocal OMIT has emerged as a prominent research area due to its unique ability to unidirectionally manipulate light-matter interactions [35,36]. Hafezi *et al.* studied the nonreciprocal transmission based on OMIT in a microring resonator by using a unidirectional optical pump [37]. Liu *et al.* discussed the nonreciprocal transmission and the fast-slow light effects in the cavity optomechanical system with different parameter conditions [38]. Xu *et al.* propose the creation of optical nonreciprocity in a three-mode optomechanical system, consisting of two linearly coupled Fabry-Pérot cavities with a membrane in the node of one of the optical cavities or a photonic crystal cavity with an optomechanical crystal [39]. They have also conducted a comprehensive numerical analysis to investigate the effects of the parameters on the nonreciprocal response of the system. The aforementioned research primarily focused on the design of various single- or double-cavity systems to investigate the nonreciprocal OMIT phenomenon, which can play an important role in optical information processing by serving as optical diodes, isolators, etc. Inspired by these studies, in this paper, we propose an approach of twofold nonreciprocal OMIT in a three-cavity system, in which the transmission characteristics of the two subpaths can be manipulated simultaneously by changing the propagating direction of the control light. In addition, the three-cavity system outperforms the two-cavity system in terms of the phenomenon of OMIT. The proposed system exhibits functionality akin to that of a single-pole double-throw (SPDT) switch or an ideal optical SPDT-type isolator, rendering it highly suitable for deployment as an optical switch within intricate networks of optical information processing. It holds potential applications in quantum information processing.

The remainder of the paper is organized as follows: In Sec. II, we introduce the model of the three-cavity optomechanical system and provide its Hamiltonian and the

\*Contact author: [yulin@ybu.edu.cn](mailto:yulin@ybu.edu.cn)

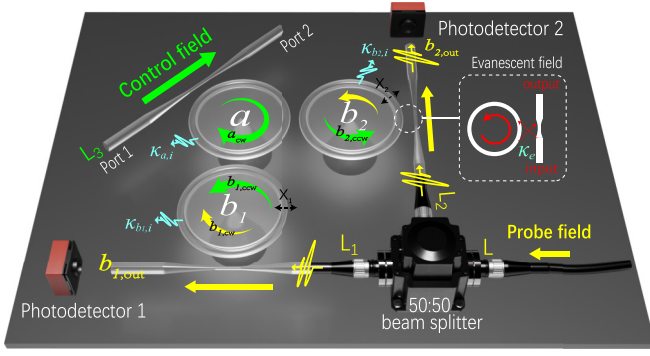


FIG. 1. Schematic diagram of our proposed model in mode I. Three WGM microresonator cavities support the CW circulating mode and the CCW circulating mode. Both of the two-cavity modes ( $b_1$ ,  $b_2$ ) couple with the mechanical mode via the radiation pressure, while cavity  $a$  is considered as a pure optical cavity. The control fields and probe fields couple with the cavity modes by an optical fiber. The antisymmetric transmission: The probe field is transmitted in path  $L_2$ , while the probe field is blocking up in path  $L_1$ .

corresponding Langevin equations. We discuss the feasibility of the proposed model and numerical results in Sec. III. Finally, a conclusion is given in Sec. IV.

## II. MODEL AND THEORY

We consider a three-cavity optomechanical system in Fig. 1, consisting of three whispering-gallery-mode (WGM) microresonators  $a$ ,  $b_1$ , and  $b_2$ , which all support the clockwise (CW) circulating mode and the counterclockwise (CCW) circulating mode. The optomechanical resonators  $b_1$ ,  $b_2$  support the mechanical breathing mode induced by the radiation pressure with the frequency  $\omega_m$  and the effective mass  $m$ , while cavity  $a$  ignores the mechanical mode due to its pure optical cavity nature. Cavity  $a$  couples to two identical microresonators ( $b_1$  and  $b_2$ ), respectively. Resonators  $b_1$  and  $b_2$  are separated by a sufficient distance, ensuring that the two cavities do not directly couple with each other. The lights are coupled into microcavities  $b_1$ ,  $b_2$ , and  $a$  by tapered optical fibers  $L_1$ ,  $L_2$ , and  $L_3$ , respectively. At the junction of these two optical fibers ( $L_1$ ,  $L_2$ ), the laser beam is split into two separate beams by the 50:50 beam splitter, which ensures the propagating light from the main path  $L$  to enter subpaths  $L_1$  and  $L_2$  with equal intensity and frequency. A strong control light with frequency  $\omega_c$  is transmitted through  $L_3$ , while a weak probe light with frequency  $\omega_p$  is transmitted through  $L$ .

In our scheme, we investigate the optical response of the probe field in the system when control light is introduced through two distinct input ports. To enhance comprehension of the underlying physical mechanism, we define mode I as the scenario where the control light is input through port 1, while mode II refers to the situation where a control light is injected via port 2. Figure 1 shows the schematic diagram of our proposed model in mode I, where the control light induces CCW control photons that counterpropagate with the probe photon in the  $b_1$  cavity and copropagate with the probe photon in the  $b_2$  cavity. Reference [40] indicates that the copropagating photons can be coherently coupled with a phonon in

an optomechanical cavity, while the coupling between counterpropagating photons and the phonon is negligible due to energy conservation and momentum matching requirements imposed by an optomechanical interaction. In addition, it should be noted that the impact of material manufacturing defects has been ignored in our discussion. Therefore, in mode I, the optomechanical interaction exclusively takes place within cavity  $b_2$  while being absent in cavity  $b_1$ . In essence, the  $b_{1,\text{ccw}}$  and  $b_{1,\text{cw}}$  modes are decoupled from each other [41, 42]. However, in mode II of the system, the optomechanical interaction occurs solely within cavity  $b_1$ , thereby leading to a reversal of the situation. The system's Hamiltonian remains invariant for different modes, with only the operators' subscripts (cw and ccw, 1 and 2) exchanging. To simplify the analysis, we focus on mode I, where the Hamiltonian of the system can be written as

$$\begin{aligned}
 \hat{H} &= \hat{H}_0 + \hat{H}_{\text{int}} + \hat{H}_{\text{dr}}, \\
 \hat{H}_0 &= \hbar\omega_a \hat{a}_{\text{cw}}^\dagger \hat{a}_{\text{cw}} + \hbar\omega_{b_1} (\hat{b}_{1,\text{cw}}^\dagger \hat{b}_{1,\text{cw}} + \hat{b}_{1,\text{ccw}}^\dagger \hat{b}_{1,\text{ccw}}) \\
 &\quad + \hbar\omega_{b_2} \hat{b}_{2,\text{ccw}}^\dagger \hat{b}_{2,\text{ccw}} + \sum_{n=1,2} \left( \frac{\hat{p}_n^2}{2m_n} + \frac{1}{2} m_n \omega_m^2 \hat{x}_n^2 \right), \\
 \hat{H}_{\text{int}} &= \sum_{n=1,2} \hbar J_n (\hat{a}_{\text{cw}}^\dagger \hat{b}_{n,\text{ccw}} + \hat{a}_{\text{cw}} \hat{b}_{n,\text{ccw}}^\dagger) \\
 &\quad + \sum_{n=1,2} \hbar G_n \hat{b}_{n,\text{ccw}}^\dagger \hat{b}_{n,\text{ccw}} \hat{x}_n, \\
 \hat{H}_{\text{dr}} &= i\hbar \sqrt{\eta \kappa_a} (\varepsilon_c \hat{a}_{\text{cw}}^\dagger e^{-i\omega_c t} - \text{H.c.}) \\
 &\quad + i\hbar \sqrt{\eta \kappa_{b_1}} (\varepsilon_p \hat{b}_{1,\text{cw}}^\dagger e^{-i\omega_p t} - \text{H.c.}) \\
 &\quad + i\hbar \sqrt{\eta \kappa_{b_2}} (\varepsilon_p \hat{b}_{2,\text{ccw}}^\dagger e^{-i\omega_p t} - \text{H.c.}), \tag{1}
 \end{aligned}$$

where  $\hat{a}_{\text{cw}}$  and  $\hat{b}_{n,\text{cw}}$  ( $\hat{b}_{n,\text{ccw}}$ ) denote the bosonic operators of the CW (CCW) optical mode, and  $\hat{x}_n$  and  $\hat{p}_n$  are the position and momentum operator of the resonator  $b_n$ .  $\omega_a$  ( $\omega_{b_n}$ ) and  $\omega_{m_n}$  are the frequencies of the cavity and mechanical modes, respectively.  $J_n$  is the effective interaction strength between cavity modes  $a_{\text{cw}}$  and  $b_{n,\text{ccw}}$ , which can be tuned by changing the distance between them.  $G_n$  is the optomechanical coupling rate of cavity  $b_n$ . The strong control field with frequency  $\omega_c$  and a weak probe field with frequency  $\omega_p$  are used to drive the optical cavities, and the amplitude of the pump field (probe field) is  $\varepsilon_c = \sqrt{P_c/\hbar\omega_c}$  ( $\varepsilon_p = \sqrt{P_p/\hbar\omega_p}$ ), where  $P_c$  ( $P_p$ ) is the control (probe) field power. The optical mode is characterized by a total loss rate  $\kappa = \kappa_i + \kappa_e$  and the cavity coupling parameter  $\eta = \kappa_e/(\kappa_i + \kappa_e)$  ( $\kappa$  is specifically manifested  $\kappa_a$  and  $\kappa_{b_n}$ ), where  $\kappa_i$  and  $\kappa_e$  denote the intrinsic and external loss rate [34].

In the frame rotating at the drive frequency  $\omega_c$ , the quantum Langevin equations of the three-cavity optomechanical system can be obtained as

$$\begin{aligned}
 \dot{\hat{a}}_{\text{cw}} &= -\left(i\Delta_a + \frac{\kappa_a}{2}\right) \hat{a}_{\text{cw}} - iJ_1 \hat{b}_{1,\text{ccw}} - iJ_2 \hat{b}_{2,\text{ccw}} \\
 &\quad + \sqrt{\eta \kappa_a} \varepsilon_c + \sqrt{\kappa_a} \hat{a}_{\text{cw},\text{in}}, \\
 \dot{\hat{b}}_{1,\text{ccw}} &= -\left(i\Delta_{b_1} + \frac{\kappa_{b_1}}{2}\right) \hat{b}_{1,\text{ccw}} - iJ_1 \hat{a}_{\text{cw}} \\
 &\quad + iG_{1x_1} \hat{b}_{1,\text{ccw}} + \sqrt{\kappa_{b_1}} \hat{b}_{1,\text{ccw},\text{in}},
 \end{aligned}$$

$$\begin{aligned}
\dot{\hat{b}}_{1,\text{cw}} &= -\left(i\Delta_{b_1} + \frac{\kappa_{b_1}}{2}\right)\hat{b}_{1,\text{cw}} + \sqrt{\eta\kappa_{b_1}}\varepsilon_p e^{-i\Delta t} \\
&\quad + \sqrt{\kappa_{b_1}}\hat{b}_{1,\text{cw},\text{in}}, \\
\dot{\hat{b}}_{2,\text{ccw}} &= -\left(i\Delta_{b_2} + \frac{\kappa_{b_2}}{2}\right)\hat{b}_{2,\text{ccw}} - iJ_2\hat{a}_{\text{cw}} \\
&\quad + iG_2x_2\hat{b}_{2,\text{ccw}} + \sqrt{\eta\kappa_{b_2}}\varepsilon_p e^{-i\Delta t} + \sqrt{\kappa_{b_2}}b_{2,\text{ccw},\text{in}}, \\
\ddot{\hat{x}}_1 + \gamma_{m_1}\dot{\hat{x}}_1 + \omega_{m_1}^2\hat{x}_1 &= \frac{\hbar G_1}{m_1}\hat{b}_{1,\text{ccw}}^\dagger\hat{b}_{1,\text{ccw}} + \frac{\hat{\xi}_1}{m_1}, \\
\ddot{\hat{x}}_2 + \gamma_{m_2}\dot{\hat{x}}_2 + \omega_{m_2}^2\hat{x}_2 &= \frac{\hbar G_2}{m_2}\hat{b}_{2,\text{ccw}}^\dagger\hat{b}_{2,\text{ccw}} + \frac{\hat{\xi}_2}{m_2}, \quad (2)
\end{aligned}$$

where  $\Delta_a = \omega_a - \omega_c$ ,  $\Delta_{b_n} = \omega_{b_n} - \omega_c$ , and  $\Delta = \omega_p - \omega_c$  is the detuning caused by the probe and the control field.  $\gamma_{m_n}$  and  $\kappa_a$  ( $\kappa_{b_n}$ ) are the mechanical damping rates and the decay rates of the cavities.  $\hat{a}_{\text{cw},\text{in}}$  and  $\hat{b}_{n,\text{ccw},\text{in}}$  ( $\hat{b}_{1,\text{cw},\text{in}}$ ) are the input vacuum noise operators with zero mean value, and their only nonzero correlation functions are  $\langle \hat{c}_{\text{in}}(t)\hat{c}_{\text{in}}^\dagger(t') \rangle = \delta(t-t')$  (where  $\hat{c}_{\text{in}}$  denotes all input vacuum noise operators) [43].  $\hat{\xi}_n$  is the Brownian stochastic force with zero mean value and its correlation function is  $\langle \hat{\xi}_n(t)\hat{\xi}_n(t') \rangle = m_n\hbar\gamma_{m_n} \int \frac{d\omega_{m_n}}{2\pi} e^{-i\omega_{m_n}(t-t')} \omega_{m_n} [\coth(\frac{\hbar\omega_{m_n}}{2k_B T}) + 1]$  (where  $n$  denotes 1,2) [44].

Since the control field is strong enough and this strong interaction can be transmitted between the intracavity fields through intercavity coupling, we can employ a linearization approach in quantum optics for analytical comprehension. Equation (2) could be linearized by expanding each operator as a sum of its steady-state mean value and a small fluctuation, i.e.,  $\hat{\rho} = \rho_s + \delta\hat{\rho}$  ( $\hat{\rho}$  indicates the operators  $\hat{a}_{\text{cw}}$ ,  $\hat{b}_{1,\text{ccw}}$ ,  $\hat{b}_{1,\text{cw}}$ ,  $\hat{b}_{2,\text{ccw}}$ ,  $\hat{x}_1$ ,  $\hat{x}_2$ ). The dynamical behaviors of the system can be obtained by solving the equation of motion for the fluctuations around their steady-state parts. The steady-state averages can be obtained by setting the derivatives of the mean-field motion equations to zero as

$$\begin{aligned}
a_{\text{cw},s} &= \frac{-iJ_1b_{1,\text{ccw},s} - iJ_2b_{2,\text{ccw},s} + \sqrt{\eta\kappa_a}\varepsilon_c}{i\Delta_a + \frac{\kappa_a}{2}}, \\
b_{1,\text{ccw},s} &= \frac{-iJ_1a_{\text{cw},s}}{i\Delta'_{b_1} + \frac{\kappa_{b_1}}{2}}, \\
b_{1,\text{cw},s} &= 0, \\
b_{2,\text{ccw},s} &= \frac{-iJ_2a_{\text{cw},s}}{i\Delta'_{b_2} + \frac{\kappa_{b_2}}{2}}, \\
x_{1,s} &= \frac{\hbar G_1}{m_1\omega_{m_1}^2}b_{1,\text{ccw},s}^*b_{1,\text{ccw},s}, \\
x_{2,s} &= \frac{\hbar G_2}{m_2\omega_{m_2}^2}b_{2,\text{ccw},s}^*b_{2,\text{ccw},s}, \quad (3)
\end{aligned}$$

where  $\Delta'_{b_n} = \Delta_{b_n} - G_n x_{n,s}$  is the effective cavity-laser detuning. In this paper, we mainly investigate the case of an optomechanical system that is driven around the red sideband regime (i.e.,  $\Delta_a \approx \omega_m$ ). Since the probe field is much weaker than the control field, i.e.,  $\varepsilon_p \ll \varepsilon_c$ , it can be treated as a steady-state disturbance. Therefore, we consider the probe field as part of the perturbation term ( $\delta\hat{b}_{1,\text{cw}}$  and  $\delta\hat{b}_{2,\text{cw}}$ ). The manifestation of the OMIT effect is determined through

the average response of the probe field. Consequently, we associate all fluctuation operators with their corresponding expectation values while disregarding vacuum and thermal noise, which have zero expectation values. Then, by ignoring the high-order nonlinear terms of the fluctuation parts, the Langevin equations for the expectation values ( $\delta\rho$ ) of the fluctuations ( $\delta\hat{\rho}$ ) can be given as

$$\begin{aligned}
\delta\dot{a}_{\text{cw}} &= -\left(i\Delta_a + \frac{\kappa_a}{2}\right)\delta a_{\text{cw}} - iJ_1\delta b_{1,\text{ccw}} - iJ_2\delta b_{2,\text{ccw}}, \\
\delta\dot{b}_{1,\text{ccw}} &= -\left(i\Delta'_{b_1} + \frac{\kappa_{b_1}}{2}\right)\delta b_{1,\text{ccw}} - iJ_1\delta a_{\text{cw}} + iG_1\delta x_1b_{1,\text{ccw},s}, \\
\delta\dot{b}_{1,\text{cw}} &= -\left(i\Delta_{b_1} + \frac{\kappa_{b_1}}{2}\right)\delta b_{1,\text{cw}} + \sqrt{\eta\kappa_{b_1}}\varepsilon_p e^{-i\Delta t}, \\
\delta\dot{b}_{2,\text{ccw}} &= -\left(i\Delta'_{b_2} + \frac{\kappa_{b_2}}{2}\right)\delta b_{2,\text{ccw}} - iJ_2\delta a_{\text{cw}} \\
&\quad + iG_2\delta x_2b_{2,\text{ccw},s} + \sqrt{\eta\kappa_{b_2}}\varepsilon_p e^{-i\Delta t}, \\
\delta\ddot{x}_1 + \gamma_{m_1}\delta\dot{x}_1 + \omega_{m_1}^2\delta x_1 &= \frac{\hbar G_1}{m_1}(b_{1,\text{ccw},s}^*\delta b_{1,\text{ccw}} + \delta b_{1,\text{ccw}}^*b_{1,\text{ccw},s}), \\
\delta\ddot{x}_2 + \gamma_{m_2}\delta\dot{x}_2 + \omega_{m_2}^2\delta x_2 &= \frac{\hbar G_2}{m_2}(b_{2,\text{ccw},s}^*\delta b_{2,\text{ccw}} + \delta b_{2,\text{ccw}}^*b_{2,\text{ccw},s}). \quad (4)
\end{aligned}$$

To solve Eq. (4), we make the ansatz as  $\delta\rho = \rho_+ e^{-i\Delta t} + \rho_- e^{i\Delta t}$  [34]. To discuss OMIT in the present optomechanical systems, we need only investigate the response of the probe field. Each operator can be expanded into multiple Fourier components by using the ansatz, and the higher-order terms are neglected under the limitation of a weak probe field. We have

$$\begin{aligned}
a_{\text{cw},+} &= \frac{-iJ_1b_{1,\text{ccw},+} - iJ_2b_{2,\text{ccw},+}}{i\Delta_a + \frac{\kappa_a}{2} - i\Delta}, \\
a_{\text{cw},-} &= \frac{-iJ_1b_{1,\text{ccw},-} - iJ_2b_{2,\text{ccw},-}}{i\Delta_a + \frac{\kappa_a}{2} + i\Delta}, \\
b_{1,\text{ccw},+} &= \frac{-iJ_1a_{\text{cw},+} + iG_1x_{1,+}b_{1,\text{ccw},s}}{i\Delta'_{b_1} + \frac{\kappa_{b_1}}{2} - i\Delta}, \\
b_{1,\text{ccw},-} &= \frac{-iJ_1a_{\text{cw},-} + iG_1x_{1,-}b_{1,\text{ccw},s}}{i\Delta'_{b_1} + \frac{\kappa_{b_1}}{2} + i\Delta}, \\
b_{1,\text{cw},+} &= \frac{\sqrt{\eta\kappa_{b_1}}\varepsilon_p}{i\Delta_{b_1} + \frac{\kappa_{b_1}}{2} - i\Delta}, \quad b_{1,\text{cw},-} = 0, \\
b_{2,\text{ccw},+} &= \frac{-iJ_2a_{\text{cw},+} + iG_2x_{2,+}b_{2,\text{ccw},s} + \sqrt{\eta\kappa_{b_2}}\varepsilon_p}{i\Delta'_{b_2} + \frac{\kappa_{b_2}}{2} - i\Delta}, \\
b_{2,\text{ccw},-} &= \frac{-iJ_2a_{\text{cw},-} + iG_2x_{2,-}b_{2,\text{ccw},s}}{i\Delta'_{b_2} + \frac{\kappa_{b_2}}{2} + i\Delta}, \\
x_{1,+} &= \frac{\hbar G_1(b_{1,\text{ccw},-}^*b_{1,\text{ccw},+} + b_{1,\text{ccw},+}b_{1,\text{ccw},-}^*)}{m_1(-\Delta^2 - i\Delta\gamma_{m_1} + \omega_{m_1}^2)}, \\
x_{1,-} &= \frac{\hbar G_1(b_{1,\text{ccw},+}^*b_{1,\text{ccw},-} + b_{1,\text{ccw},-}b_{1,\text{ccw},+}^*)}{m_1(-\Delta^2 + i\Delta\gamma_{m_1} + \omega_{m_1}^2)},
\end{aligned}$$

$$\begin{aligned}
 x_{2,+} &= \frac{\hbar G_2 (b_{2,\text{ccw}}^* - b_{2,\text{ccw},s} + b_{2,\text{ccw}} + b_{2,\text{ccw},s}^*)}{m_2 (-\Delta^2 - i\Delta\gamma_{m_2} + \omega_{m_2}^2)}, \\
 x_{2,-} &= \frac{\hbar G_2 (b_{2,\text{ccw}}^* + b_{2,\text{ccw},s} + b_{2,\text{ccw}} - b_{2,\text{ccw},s}^*)}{m_2 (-\Delta^2 + i\Delta\gamma_{m_2} + \omega_{m_2}^2)}, \quad (5)
 \end{aligned}$$

Due to the complete similarity of cavities  $b_1$  and  $b_2$  in the considered three-cavity system, implying identical parameters ( $\omega_{b_n}$ ,  $\omega_{m_n}$ ,  $m_n$ ,  $J_n$ ,  $G_n$ ,  $\kappa_{b_n}$ ,  $\gamma_{m_n}$ ), we unify these parameters above by removing the subscript “ $n$ .” Considering that the optomechanical interaction is predominantly governed by the control field, we can obtain the same  $\hat{x}_1$  and  $\hat{x}_2$  (i.e.,  $\Delta'_b = \Delta'_b$ ). Solving the set of Eq. (5), we approximatively obtain

$$\begin{aligned}
 b_{2,\text{ccw},+} &= \frac{\sqrt{\eta\kappa_{b_2}\varepsilon_p}}{\Lambda_1 + \Lambda_2 - \Lambda_3}, \quad \Lambda_1 = i\Delta'_b + \frac{\kappa_b}{2} - i\Delta, \\
 \Lambda_2 &= \frac{2J^2}{i\Delta_a + \frac{\kappa_a}{2} - i\Delta}, \\
 \Lambda_3 &= \frac{i\hbar G^2 \frac{1}{1-M} |b_{2,\text{ccw},s}|^2}{m(-\Delta^2 - i\Delta\gamma_m + \omega_m^2)}, \quad (6)
 \end{aligned}$$

where  $M = i\hbar G^2 / [m(-\Delta^2 - i\Delta\gamma_m + \omega_m^2)(i\Delta'_b - \kappa_b/2 + i\Delta + \frac{2J^2}{i\Delta_a - \kappa_a/2 + i\Delta})]$  ( $\Delta'_b$  denotes  $\Delta'_b$  and  $\Delta'_b$ ).

Subsequently, we focus on the output field of the probe laser received by the detectors. Combining with the standard input-output relation  $c_{\text{out}}(t) = c_{\text{in}}(t) - \sqrt{\eta\kappa}c(t)$  [43], we have

$$\begin{aligned}
 c_{\text{out}} &= (\varepsilon_c - \sqrt{\eta\kappa}c_s)e^{-i\omega_c t} + (\varepsilon_p - \sqrt{\eta\kappa}c_+)e^{-i(\omega_c + \Delta)t} \\
 &\quad - \sqrt{\eta\kappa}c_- e^{-i(\omega_c - \Delta)t}, \quad (7)
 \end{aligned}$$

where  $c$  denotes the modes  $b_{1,\text{cw}}$  and  $b_{2,\text{ccw}}$  ( $\kappa$  denotes  $\kappa_{b_1}$  and  $\kappa_{b_2}$ , and  $\kappa_{b_1} = \kappa_{b_2}$ ), and the transmission of the probe field is then given by

$$T_{c_{\text{out}}} = |t(\omega_s)|^2 = \left| \frac{c_{\text{out}}(t)}{c_{\text{in}}(t)} \right|^2 = \left| 1 - \frac{\sqrt{\eta\kappa}c_+}{\varepsilon_p} \right|^2, \quad (8)$$

where  $c_+$  represents the output field at the probe frequency, and  $c_-$  shows the nonlinear generated field for control field, probe field and mechanical oscillator in a four-wave mixing process, which is not displayed here.

### III. NUMERICAL RESULTS AND ANALYSIS

In this section, we numerically evaluate both the transmission rates  $T_{b_1,\text{cw}}$  and  $T_{b_2,\text{ccw}}$ , for different input ports of the control field, to demonstrate the twofold nonreciprocal transmissions of the probe field. Furthermore, we explore the possibility of the three-cavity optomechanical system as an optical SPDT switch or an optical SPDT-like isolator.

We adopt experimentally feasible parameters [45–47], i.e.,  $m = 2$  ng,  $\omega_m = 200$  MHz,  $\gamma_m = 0.2$  MHz, the wavelength of the laser  $\lambda = 1.55$   $\mu\text{m}$ , refractive index  $N = 1.44$ ,  $\omega_a = \omega_b = 193.5$  THz. We consider  $\Delta_a \approx \Delta'_b \approx \omega_m$ , the quality factor of the optical resonator  $Q = 3 \times 10^7$ ,  $\kappa_e = \kappa_i = \omega/Q$  (where  $\omega$  denotes  $\omega_a$  and  $\omega_b$ ,  $\eta = 1/2$ ),  $P_c = 10$  W,  $r = 0.25$  mm ( $r$  is the radius of the microresonator), and  $G = \omega/r$ . The system is in the resolved-sideband regime with  $\kappa \ll \omega_m$ . The probe field frequency for both resonators (cavities  $b_n$ ) is identical, owing to the presence of the beam splitter. We set  $J = \kappa$

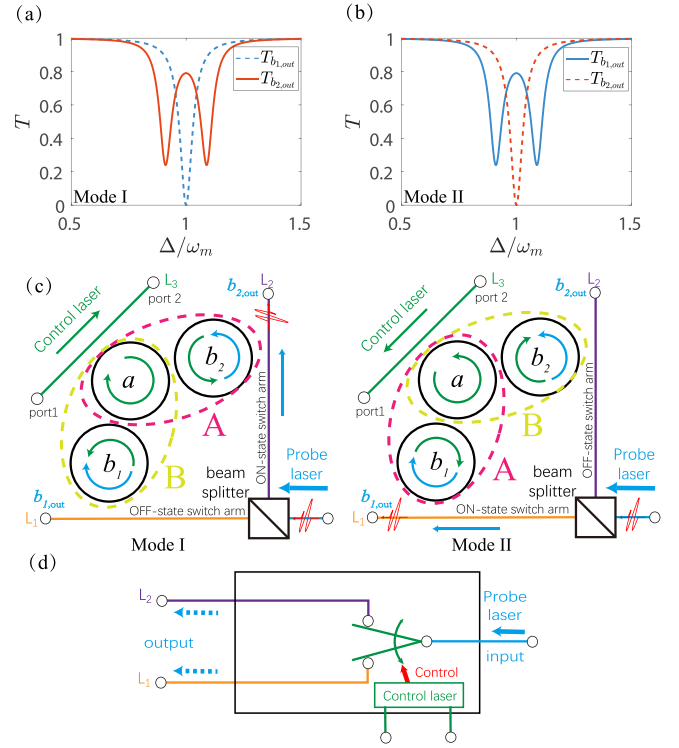


FIG. 2. The probe transmission rate as a function of the detuning  $\Delta/\omega_m$  in (a) mode I and (b) mode II. (c) The schematic of twofold nonreciprocity in the three-cavity system. (d) The schematic diagram of the single-pole double-throw switch approximated by the system.

(i.e.,  $J = 2\kappa_e$ ), and introduce the reference unit  $\mathcal{V} = 12.9$  MHz for convenience. The strength of parameter  $J$  can be controlled by altering the separation between the resonators. Peng *et al.* have experimentally shown that reducing the gap between two resonators to approximately 5  $\mu\text{m}$  establishes strong inter-resonator coupling, as reported in Refs. [47,48].

Figure 2(a) plots the transmission rate  $T$  of the probe light as a function of the probe-control field detuning  $\Delta/\omega$  for the resonator  $b_1$  and  $b_2$  in mode I, respectively. In the cavity  $b_1$ , the coupling of the probe light with the phonon is negligible, which allows the cavity to maintain the absorption of the probe light, which is displayed by the blue dashed curve. The red solid curve presents the famous phenomenon of OMIT in cavity  $b_2$  due to the optomechanical interaction. Additionally, Fig. 2(b) illustrates the characterization in mode II.

As depicted in Fig. 2(c), for an effective demonstration of the system’s nonreciprocity, we can partition this axisymmetric structure into two distinct regions, A and B (region A, where the control field propagates in the same direction as the probe field within cavity  $b_n$ , and region B, where the control field propagates counter to the probe field within cavity  $b_n$ ). In region A, a transparency window is observed for the probe light. Conversely, in region B, strong absorption of the probe light is exhibited. Alternatively, when the control light is input from port 1 (mode I),  $L_1$  acts as a blocking path, whereas when the control light is input from port 2 (mode II),  $L_1$  transforms into the transmission path. The same principle applies to  $L_2$ . Based on the preceding discussion, it is evident that our scheme exhibits nonreciprocity, denoting the asymmetric

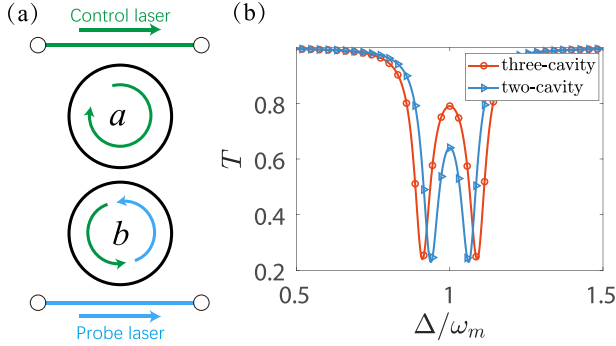


FIG. 3. (a) Two-cavity optomechanical system model. (b) The probe transmission rate  $T$  as a function of the detuning  $\Delta/\omega_m$  for different optomechanical systems.

response of the transmission channel when altering the injection direction of the control light [49–53]. Interestingly, regardless of the input direction of the control light, both  $L_1$  and  $L_2$  consistently exhibit asymmetric transmission responses. Given this inherent pairwise nonreciprocity within our system configuration, we consider it to manifest twofold nonreciprocity. Moreover, the structure of this system is formally equivalent to an SPDT switch, where  $L_1$  and  $L_2$  resemble the off-state and on-state switch arms of the SPDT switch, as depicted in Fig. 2(d).

It is noteworthy that this three-cavity system outperforms the two-cavity system [as shown in Fig. 3(a)]. According to the aforementioned description, enhancing the destructive interference effect between the anti-Stokes photons and probe photons is an effective approach for improving the OMIT effect. In the two-cavity system, anti-Stokes photons scattered from cavity  $b$  interfere destructively with the probing photons. However, in the three-cavity system, the scattering process of the control photons occurs simultaneously in cavities  $b_1$  and  $b_2$ , resulting in a higher number of anti-Stokes photons compared to the two-cavity system. Due to the indirect coupling between cavity  $b_1$  and cavity  $b_2$  through cavity  $a$  [via the Hamiltonian form  $\sum_{n=1,2} \hbar J_n (\hat{a}_{cw}^\dagger \hat{b}_{n,ccw} + \hat{a}_{cw} \hat{b}_{n,ccw}^\dagger)$  in mode I or  $\sum_{n=1,2} \hbar J_n (\hat{a}_{ccw}^\dagger \hat{b}_{n,cw} + \hat{a}_{ccw} \hat{b}_{n,cw}^\dagger)$  in mode II], probing photons possess pathways for interfering with significantly more photons within the three-cavity system. Therefore, the OMIT phenomenon exhibits greater superiority in the three-cavity

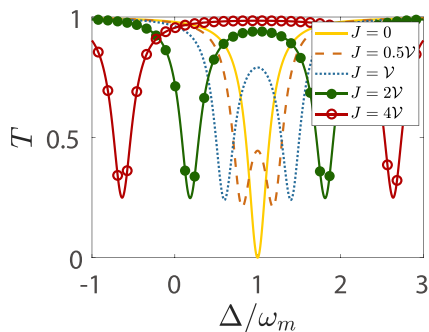


FIG. 4. The probe transmission rate  $T$  as a function of the detuning  $\Delta/\omega_m$  for different  $J$  in cavity  $b_2$ .

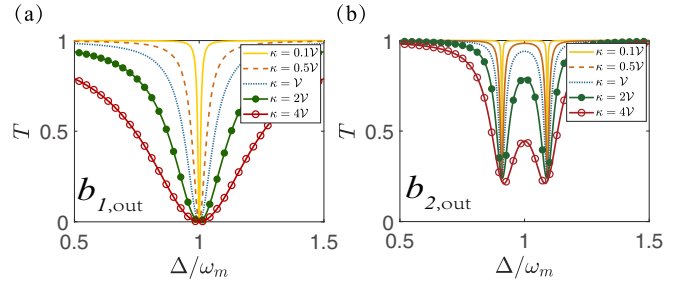


FIG. 5. The probe transmission rate  $T$  as a function of the detuning  $\Delta/\omega_m$  with increasing loss rate  $\kappa$  in (a) cavity  $b_1$  and (b) cavity  $b_2$ , respectively.

system compared to the two-cavity system. As illustrated in Fig. 3(b), the peak value of the transparent window in the three-cavity system surpasses that of the two-cavity system under identical initial parameters. The probe transmission rate  $T$  increases from 0.64 to 0.79 at resonance  $\Delta/\omega_m = 1$ , representing a significant enhancement of  $\sim 23.4\%$ .

We further investigated the impact of coupling strength on the system (only mode I was investigated in the following for convenience). In Fig. 4, we plot the transmission of the probe field  $T$  versus the detuning  $\Delta/\omega_m$  with different coupling strengths  $J$  in the optomechanical system. By gradually increasing the coupling strength  $J$ , the absorption properties of cavity  $b_2$  to the probe light are weakened at the resonance, resulting in a transparency window in the spectrum. This phenomenon arises due to the enhanced cavity-cavity coupling coefficient, enabling effective control light transmission from cavity  $a$  to cavity  $b_2$ , thereby promoting the destructive interference effect between the control light and the probe field. Hence there will be an enhancement of the OMIT phenomena.

The loss rate also exerts an influence on the system. In Figs. 5(a) and 5(b), we display the probe transmission rate  $T$  as a function of the detuning  $\Delta/\omega_m$  with increasing loss rate  $\kappa$  (set  $J = V$ ). As the loss rate increases, it will lead to a large leakage of the probe and control photons through dissipation in cavity  $b_2$  and the transparency phenomenon of the system to the probe light will weaken gradually in cavity  $b_2$ . Meanwhile, the leakage of cavity  $b_1$  results in a low probe transmission rate.

As previously described, twofold nonreciprocal OMIT has been observed in a three-cavity optomechanical system, which is formally equivalent to a SPDT switch or SPDT-like isolator. We propose three parameters to evaluate the nonreciprocity of

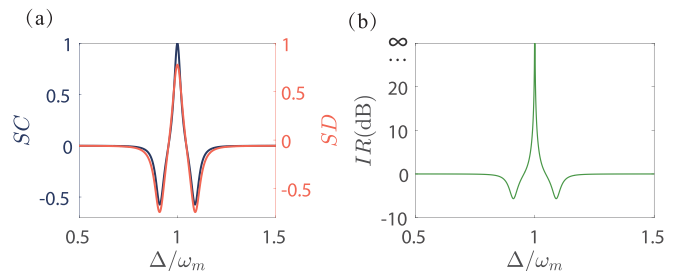


FIG. 6. (a) The  $SC$ ,  $SD$  and (b)  $IR$  vs the detuning  $\Delta/\omega_m$  for  $J = \kappa = V$ .

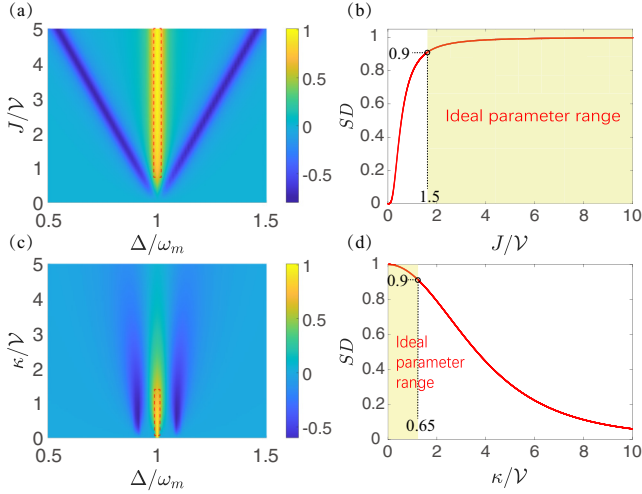


FIG. 7. The probe transmission rate  $T$  as a function of the detuning  $\Delta/\omega_m$  with increasing (a) coupling strength  $J$  and (c) loss rate  $\kappa$  in cavity  $b_2$ , respectively. The SD vs (b) coupling strength  $J$  and (d) loss rate  $\kappa$  at the resonance  $\Delta/\omega_m = 1$ .

the subpaths in the system (we only investigate cavity  $b_1$  in following for convenience): switching contrast (SC), switching difference (SD), and isolation ratio (IR) [54,55]. We have

$$\begin{aligned} \text{SC} &= \frac{T_{\text{ON}} - T_{\text{OFF}}}{T_{\text{ON}} + T_{\text{OFF}}} = \frac{T_{b_{1,\text{mode II}}} - T_{b_{1,\text{mode I}}}}{T_{b_{1,\text{mode II}}} + T_{b_{1,\text{mode I}}}}, \\ \text{SD} &= T_{\text{ON}} - T_{\text{OFF}} = T_{b_{1,\text{mode II}}} - T_{b_{1,\text{mode I}}}, \\ \text{IR} &= 10 \log_{10} (T_{\text{ON}}/T_{\text{OFF}}) \\ &= 10 \log_{10} (T_{b_{1,\text{mode II}}}/T_{b_{1,\text{mode I}}}). \end{aligned} \quad (9)$$

Figures 6(a) and 6(b) plot SC, SD, and IR of the systems. It is demonstrated that both SC and IR have ideal values ( $\text{SC} \sim 1$ ,  $\text{IR} \sim \infty$ ) at  $\Delta \simeq \omega_m$ . It means that the system could be considered as an ideal SPDT switch. We mainly investigate SD at  $\Delta \simeq \omega_m$ , as a symbol for quantification of the switch for later discussion.

Figures 7(a) and 7(c) show the SD against detuning  $\Delta/\omega_m$  and coupling strength  $J$  (loss rate  $\kappa$ ), while Figs. 7(b) and 7(d) highlight the parts of Figs. 7(a) and 7(c) at resonance  $\Delta = \omega_m$ . In Figs. 7(a) and 7(c), the regions where  $\text{SD} \geq 0.9$  are highlighted with dashed lines. It means that an appropriate value of the coupling strength  $J$  and loss rate  $\kappa$  meet our requirements. As shown in Figs. 7(b) and 7(d), it can be observed that with an increase of coupling strength  $J$ , the SD increases. The SD approaches 0.9 at  $\Delta = \omega_m$ , when  $J \approx 1.5\gamma$ , particularly. With an increase of the loss rate  $\kappa$ , the SD decreases. The SD

approaches 0.9 at  $\Delta = \omega_m$ , when  $\kappa \approx 0.65\gamma$ , which satisfies our expectations for the application of this model in optical switch systems.

#### IV. DISCUSSION AND CONCLUSIONS

Based on the aforementioned analysis, it is evident that a transparent window emerges in the transmission spectrum of the probe light influenced by the optomechanical interaction, known as OMIT. The transparency of OMIT should be distinguished from Autler-Townes splitting (ATS) transparency. OMIT is regarded as analogous to EIT which is based on quantum destructive interference near the resonant frequency. However, the transparent window of ATS is created by the superposition of two separate Lorentz-like absorption lines near the resonant frequency. Numerous studies have extensively examined the differences between EIT and ATS phenomena [56–59]. Our proposal is based on the phenomenon of destructive interference between anti-Stokes photons and probe photons, which arises from the optomechanical interaction. Consequently, we have achieved OMIT by employing a mechanism distinct from ATS.

In conclusion, we investigated the phenomenon of twofold nonreciprocal OMIT in a three-cavity optomechanical system. By manipulating the propagating direction of the driving laser, we achieve simultaneous control over two branch paths, enabling selective transmission along one path while consistently blocking the other. This SPDT-like characteristic enhances the performance of our system as an optical switch compared to a conventional switch limited to controlling only one optical path. Additionally, the optomechanical switch demonstrates the system's selectivity towards the frequency of the incident light near the transparent window. The reduced half width of the transparent window enhances the system's sensitivity to minute changes in frequency, thereby endowing the switch with superior tunability and heightened sensitivity. Moreover, this optomechanical switch operates based on optomechanical interaction principles and holds potential applications in various domains such as sensing weak force interactions. This design holds great potential for applications in optical communication networks and quantum technologies. Furthermore, we have shown that the three-cavity optomechanical system exhibits a superior OMIT phenomenon to the two-cavity optomechanical system due to indirect coupling and excellent nonreciprocity under certain parameter conditions (high coupling strength  $J_n$  and low loss rate  $\kappa$ ).

#### ACKNOWLEDGMENT

This work was supported by the National Natural Science Foundation of China under Grant No. 12264051.

[1] M. Aspelmeyer, T. J. Kippenberg, and F. Marquardt, *Rev. Mod. Phys.* **86**, 1391 (2014).  
 [2] T. J. Kippenberg and K. J. Vahala, *Science* **321**, 1172 (2008).  
 [3] F. Marquardt and S. M. Girvin, *Physics* **2**, 40 (2009).  
 [4] P. Verlot, A. Tavernarakis, T. Briant, P. F. Cohadon, and A. Heidmann, *Phys. Rev. Lett.* **104**, 133602 (2010).

[5] S. Mahajan, T. Kumar, A. B. Bhattacharjee, and ManMohan, *Phys. Rev. A* **87**, 013621 (2013).  
 [6] S. Gigan, H. Böhm, M. Paternostro, F. Blaser, G. Langer, J. Hertzberg, K. C. Schwab, D. Bäuerle, M. Aspelmeyer, and A. Zeilinger, *Nature (London)* **444**, 67 (2006).

- [7] O. Arcizet, P. F. Cohadon, T. Briant, M. Pinard, and A. Heidmann, *Nature (London)* **444**, 71 (2006).
- [8] T. J. Kippenberg, H. Rokhsari, T. Carmon, A. Scherer, and K. J. Vahala, *Phys. Rev. Lett.* **95**, 033901 (2005).
- [9] M. Tomes and T. Carmon, *Phys. Rev. Lett.* **102**, 113601 (2009).
- [10] X. Jiang, Q. Lin, J. Rosenberg, K. Vahala, and O. Painter, *Opt. Express* **17**, 20911 (2009).
- [11] J. Thompson, B. Zwickl, A. Jayich, F. Marquardt, S. Girvin, and J. Harris, *Nature (London)* **452**, 72 (2008).
- [12] A. Jayich, J. Sankey, B. Zwickl, C. Yang, J. Thompson, S. Girvin, A. Clerk, F. Marquardt, and J. Harris, *New J. Phys.* **10**, 095008 (2008).
- [13] J. C. Sankey, C. Yang, B. M. Zwickl, A. M. Jayich, and J. G. Harris, *Nat. Phys.* **6**, 707 (2010).
- [14] M. Karuza, C. Biancofiore, M. Bawaj, C. Molinelli, M. Galassi, R. Natali, P. Tombesi, G. Di Giuseppe, and D. Vitali, *Phys. Rev. A* **88**, 013804 (2013).
- [15] C. Regal, J. Teufel, and K. Lehnert, *Nat. Phys.* **4**, 555 (2008).
- [16] J. D. Teufel, D. Li, M. S. Allman, K. Cicak, A. Sirois, J. D. Whittaker, and R. Simmonds, *Nature (London)* **471**, 204 (2011).
- [17] F. Marquardt, J. P. Chen, A. A. Clerk, and S. M. Girvin, *Phys. Rev. Lett.* **99**, 093902 (2007).
- [18] I. Wilson-Rae, N. Nooshi, W. Zwerger, and T. J. Kippenberg, *Phys. Rev. Lett.* **99**, 093901 (2007).
- [19] Y. C. Liu, Y. F. Xiao, X. Luan, and C. W. Wong, *Phys. Rev. Lett.* **110**, 153606 (2013).
- [20] D. Y. Wang, C. H. Bai, S. Liu, S. Zhang, and H. F. Wang, *Phys. Rev. A* **98**, 023816 (2018).
- [21] D. Stefanatos, *Automatica* **73**, 71 (2016).
- [22] B. He, L. Yang, Q. Lin, and M. Xiao, *Phys. Rev. Lett.* **118**, 233604 (2017).
- [23] J. Li, G. Li, S. Zippilli, D. Vitali, and T. Zhang, *Phys. Rev. A* **95**, 043819 (2017).
- [24] J. Q. Liao, Q. Q. Wu, and F. Nori, *Phys. Rev. A* **89**, 014302 (2014).
- [25] D. Vitali, S. Gigan, A. Ferreira, H. R. Böhm, P. Tombesi, A. Guerreiro, V. Vedral, A. Zeilinger, and M. Aspelmeyer, *Phys. Rev. Lett.* **98**, 030405 (2007).
- [26] D. Stefanatos, *Quantum Sci. Technol.* **2**, 014003 (2017).
- [27] S. Gröblacher, K. Hammerer, M. R. Vanner, and M. Aspelmeyer, *Nature (London)* **460**, 724 (2009).
- [28] J. M. Dobrindt, I. Wilson-Rae, and T. J. Kippenberg, *Phys. Rev. Lett.* **101**, 263602 (2008).
- [29] S. Huang and G. S. Agarwal, *Phys. Rev. A* **80**, 033807 (2009).
- [30] L. Chen, W. Wu, F. Huang, Y. Chen, G. S. Liu, Y. Luo, and Z. Chen, *Phys. Rev. A* **105**, L031501 (2022).
- [31] F. Huang, L. Chen, L. Huang, J. Huang, G. Liu, Y. Chen, Y. Luo, and Z. Chen, *Phys. Rev. A* **104**, L031503 (2021).
- [32] L. Chen, F. Huang, H. Wang, L. Huang, J. Huang, G. S. Liu, Y. Chen, Y. Luo, and Z. Chen, *Chaos Solit. Fractals* **164**, 112678 (2022).
- [33] G. S. Agarwal and S. Huang, *Phys. Rev. A* **81**, 041803(R) (2010).
- [34] S. Weis, R. Rivière, S. Deléglise, E. Gavartin, O. Arcizet, A. Schliesser, and T. J. Kippenberg, *Science* **330**, 1520 (2010).
- [35] X. W. Xu and Y. Li, *Phys. Rev. A* **91**, 053854 (2015).
- [36] B. He, L. Yang, X. Jiang, and M. Xiao, *Phys. Rev. Lett.* **120**, 203904 (2018).
- [37] M. Hafezi and P. Rabl, *Opt. Express* **20**, 7672 (2012).
- [38] J. H. Liu, Y. F. Yu, and Z. M. Zhang, *Opt. Express* **27**, 15382 (2019).
- [39] X. W. Xu, L. N. Song, Q. Zheng, Z. H. Wang, and Y. Li, *Phys. Rev. A* **98**, 063845 (2018).
- [40] Z. Shen, Y. L. Zhang, Y. Chen, C. L. Zou, Y. F. Xiao, X. B. Zou, F.-W. Sun, G. C. Guo, and C. H. Dong, *Nat. Photon.* **10**, 657 (2016).
- [41] X. Guo, C. L. Zou, H. Jung, and H. X. Tang, *Phys. Rev. Lett.* **117**, 123902 (2016).
- [42] Y. Chen, Y. L. Zhang, Z. Shen, C. L. Zou, G.-C. Guo, and C. H. Dong, *Phys. Rev. Lett.* **126**, 123603 (2021).
- [43] C. W. Gardiner and P. Zoller, *Quantum Noise* (Springer, Berlin, 2004).
- [44] V. Giovannetti and D. Vitali, *Phys. Rev. A* **63**, 023812 (2001).
- [45] H. Guo, M. Karpov, E. Lucas, A. Kordts, M. H. Pfeiffer, V. Brasch, G. Lihachev, V. E. Lobanov, M. L. Gorodetsky, and T. J. Kippenberg, *Nat. Phys.* **13**, 94 (2017).
- [46] H. Lü, Y. Jiang, Y. Z. Wang, and H. Jing, *Photon. Res.* **5**, 367 (2017).
- [47] I. M. Mirza, W. Ge, and H. Jing, *Opt. Express* **27**, 25515 (2019).
- [48] B. Peng, Ş. K. Özdemir, J. Zhu, and L. Yang, *Opt. Lett.* **37**, 3435 (2012).
- [49] D. L. Sounas and A. Alù, *Nat. Photon.* **11**, 774 (2017).
- [50] H. Z. Shen, Q. Wang, J. Wang, and X. X. Yi, *Phys. Rev. A* **101**, 013826 (2020).
- [51] Y. Xu, J. Y. Liu, W. J. Liu, and Y. F. Xiao, *Phys. Rev. A* **103**, 053501 (2021).
- [52] Y. L. Ren, *Opt. Lett.* **47**, 1125 (2022).
- [53] Q. J. Zheng, W. X. Zhong, G. L. Cheng, and A. X. Chen, *EPJ Quantum Technol.* **11**, 8 (2024).
- [54] K. Xia and J. Twamley, *Phys. Rev. X* **3**, 031013 (2013).
- [55] C. Liang, B. Liu, A. N. Xu, X. Wen, C. Lu, K. Xia, M. K. Tey, Y. C. Liu, and L. You, *Phys. Rev. Lett.* **125**, 123901 (2020).
- [56] B. Peng, S. K. Özdemir, W. Chen, F. Nori, and L. Yang, *Nat. Commun.* **5**, 5082 (2014).
- [57] P. M. Anisimov, J. P. Dowling, and B. C. Sanders, *Phys. Rev. Lett.* **107**, 163604 (2011).
- [58] L. Chen, Y. Han, Q. Liu, Y. G. Liu, W. G. Zhang, and K. C. Chou, *Opt. Lett.* **43**, 1662 (2018).
- [59] L. Yu, L. Chen, W. G. Zhang, Y. X. Zhang, Y. S. Zhang, L. X. Kong, T. Y. Yan, and J. Q. Li, *J. Lightwave Technol.* **37**, 3620 (2019).